LBL-10972

Lawrence Berkeley Laboratory
UNIVERSITY OF CALIFORNIA

Accelerator & Fusion
Research Division

AIR FLOW INTO THE LBL BEVATRON

Jack D. Williams
(M.S. thesis)

September 1979

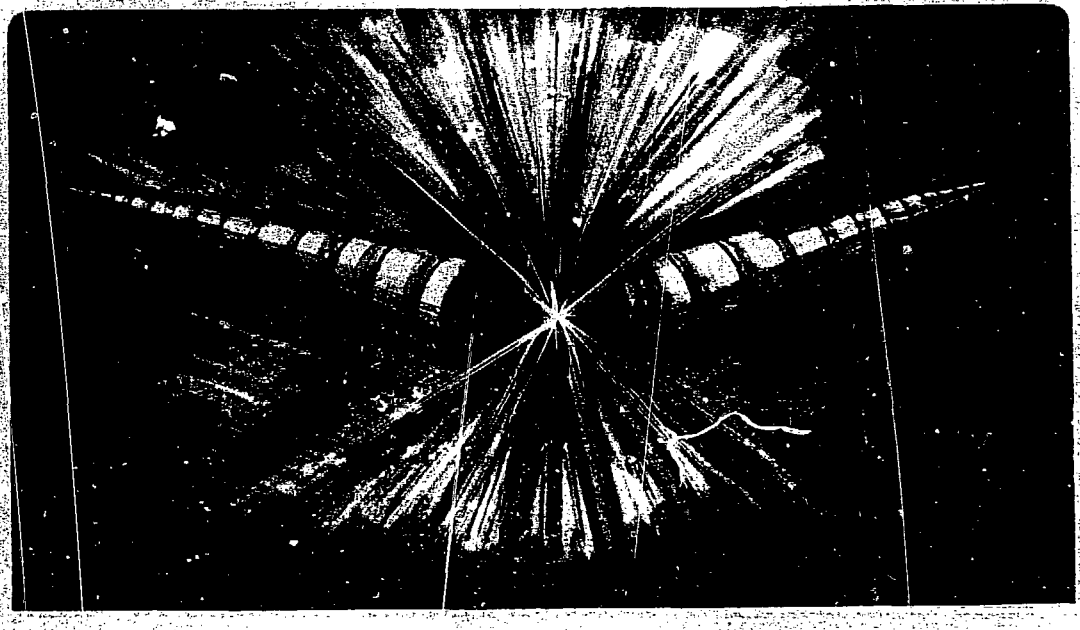

Prepared for the U.S. Department of Energy under Contract W-7405-ENG-48

AIR FLOW INTO THE

LBL BEVATRON

Jack D. Williams

Submitted Fall 79

ME 299
Professor S. Berger

TABLE OF CONTENTS

I. Objective

The Lawrence Berkeley Laboratory is currently installing an improved liner in its Bevatron. The new liner will be capable of producing a vacuum of 2×10^{-8} N/M^2 (1.5×10^{-10} Torr) and a temperature on the order of 12K. There has been concern for quite some time about possible damage to the liner in the event of a beam line window breaking allowing atmospheric air to rush into the vacuum. The installation of the new more fragile liner has heightened this concern.

This effort is an attempt to characterize the pressure loading on the cryopanel in the event of a beam window rupture. Also of interest is the time it would take the inrushing atmospheric air to reach the tangent tank where the fragile cryopanels are located. Fast acting valves placed between sections D and E at the beam line tangent tank junction are being considered as a precaution (see configuration sketches Figures 1 and 2).

II. Approach

For the initial conditions in the beam line the Knudsen number is on the order of 10^6 (see Appendix A for details of the calculation). Although this is clearly in the free molecular flow regime, continuum conservation equations are used throughout in order to render the problem tractable.

III. Beam Line Inlet

The beam line is modelled as a diaphragm separating the atmospheric stagnation reservoir from the low pressure beam line (see Figure 3). Sections A through D of the beam line are at a temperature of 295K.

Sections E and F are at 12K. At sufficiently large times after diaphragm rupture the spherical expansion wave moving into the atmospheric reservoir can be ignored and local three-dimensional diaphragm bursting effects have been damped out. Then the following six equations govern the shock flow, the contact surface, and the nozzle flow behind it. In these equations

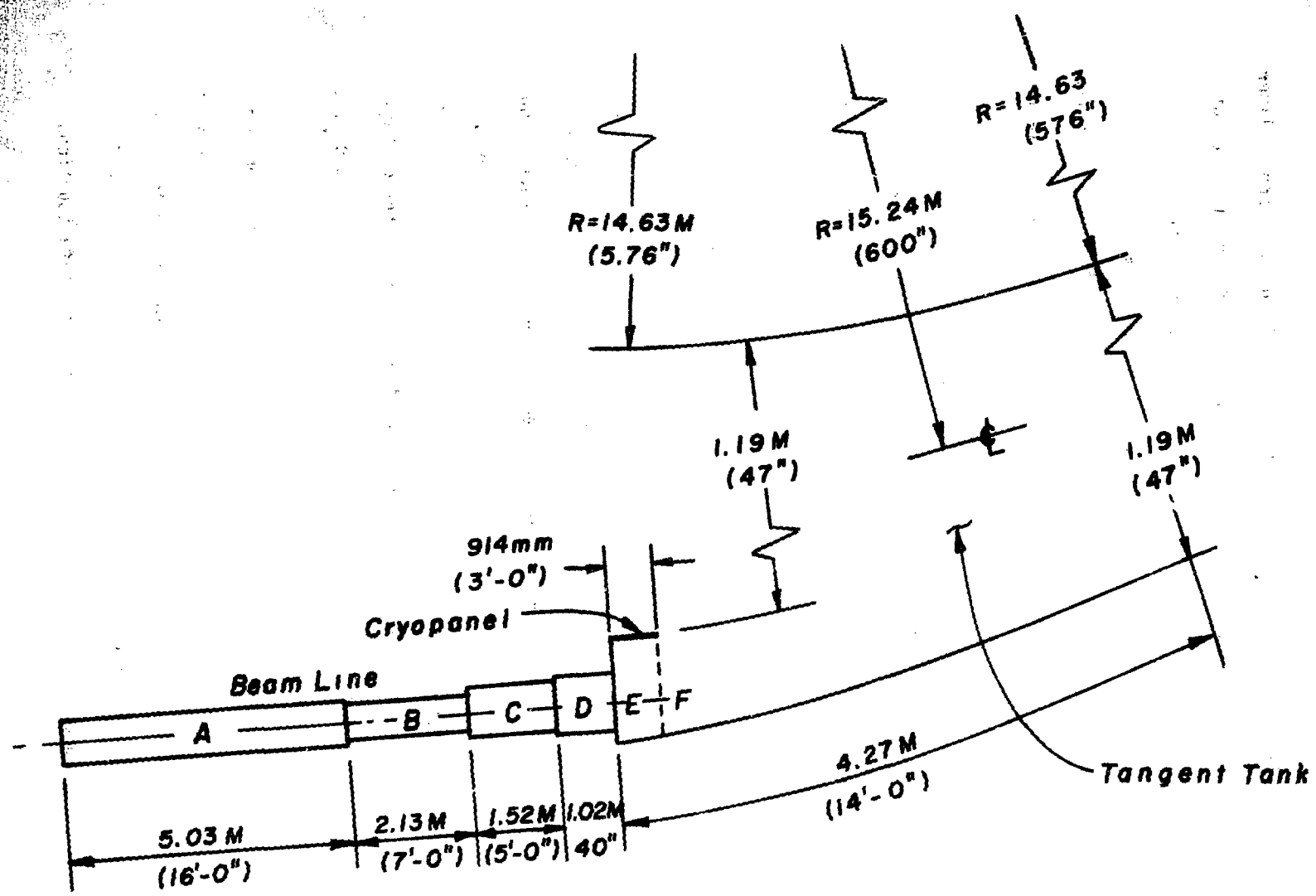

Fig. 1 PLAN VIEW

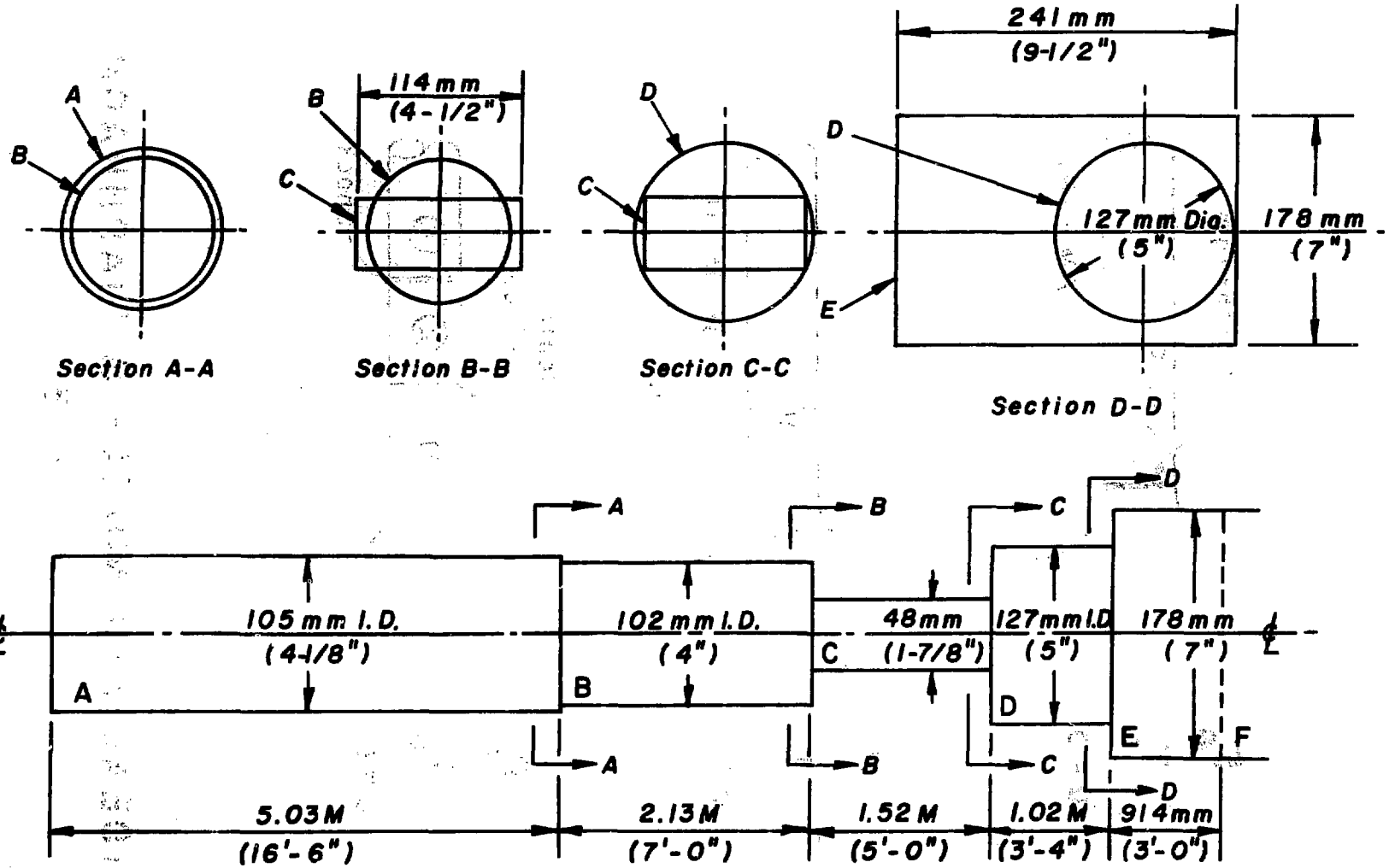

Fig. 2 ELEVATION VIEW

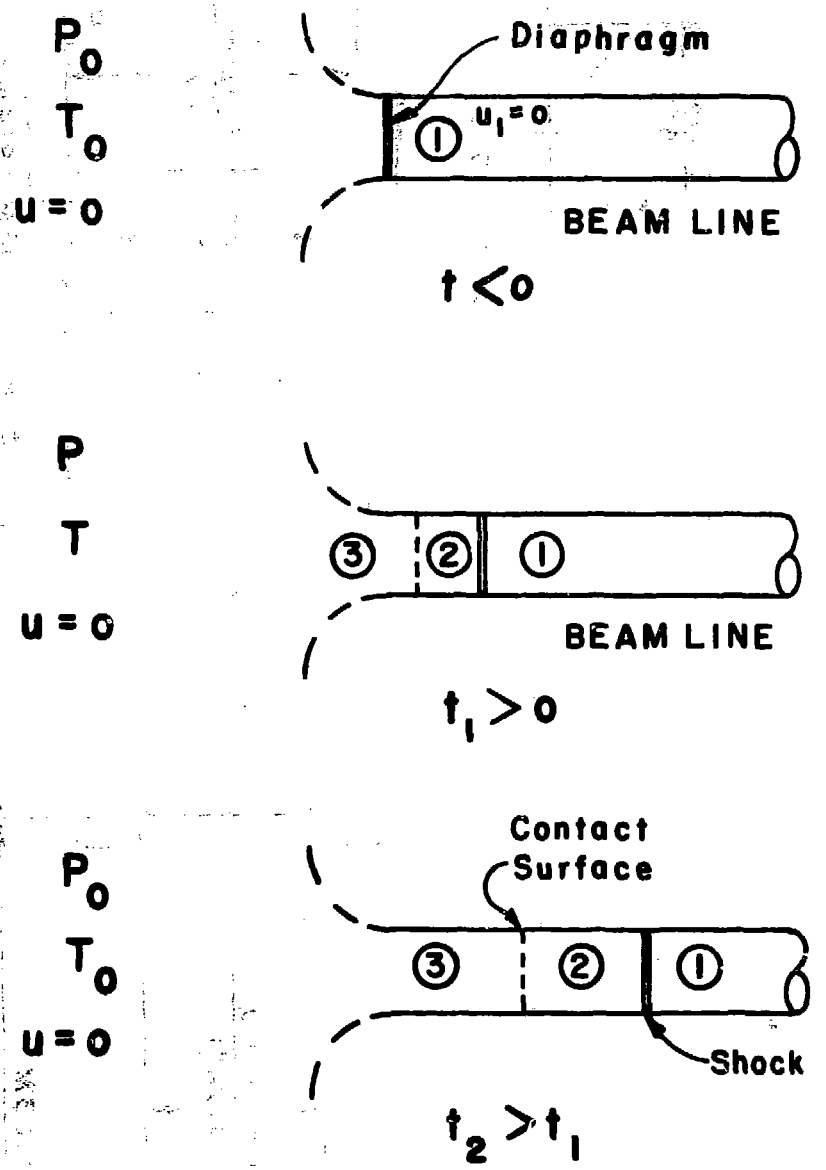

IDEALIZED NOZZLE & DIAPHRAGM

Figure 3

M_s : shock Mach number.

M_3 : region 3 flow Mach number.

P_0/P_1 : diaphragm pressure ratio.

a_0 : atmospheric stagnation sound speed.

a_1 : region 1 sound speed.

U_i : velocity in region i.

P_i : static pressure in region i.

The pressure jump produced by the shock is:

$$(1) \qquad \left(\frac{P_2}{P_1}\right)_{\text{shock}} = 1 + \frac{2\gamma}{\gamma + 1}\left(M_s^2 - 1\right) \qquad \text{(shock)}$$

The particle velocity between the shock and the contact surface (region 2) is:

$$(2) \qquad U_2 = \frac{2a_1}{\gamma + 1}\left(M_s - \frac{1}{M_s}\right) \qquad \text{(shock)}$$

Entrance effects are ignored so that isentropic flow is presumed to exist between the stagnation reservoir (state o) and the left side of the contact surface. The flow Mach number in region 3 is:

$$(3) \qquad M_3 = \frac{U_3}{a_0}\left[1 - \frac{\gamma - 1}{2}\left(\frac{U_3}{a_0}\right)^2\right]^{-1/2} \qquad \text{(isentropic)}$$

The static pressure in region 3 is:

$$(4) \qquad P_3 = P_0 \left(1 + \frac{\gamma - 1}{2} M_3^2\right)^{\frac{-\gamma}{\gamma - 1}} \qquad \text{(isentropic)}$$

By requiring mechanical equilibrium across the contact surface two additional equations are available:

$$(5) \text{ and } (6) \qquad U_2 = U_3 \quad ; \quad P_2 = P_3$$

There are now six equations and six unknowns. For the initial diaphragm pressure ratio the unique solution is given in Table 1.

Physically this is an unreasonable solution. The flow velocity in region 3 is just slightly less than the stedy state escape velocity corresponding to the reservoir stagnation conditions. Evidently the solution is dominated by the extremely low pressure into which the shock must propagate. At sufficiently large times, as discussed earlier, we are on solid ground in assuming quasi-steady choked flow. Furthermore since continuum shocks would not exist we shall relax our requirement for the existence of a shock. We shall assume that the contact surface is actually the leading edge of the choked flow and treat its particle velocity as the particle velocity behind an imaginary shock. We then have sufficient information to calculate reflected pressures.

Before completely discarding this approach let's examine the sensitivity of the solution to the diaphragm pressure ratio P_0/P_1. Figure 4 shows the

Table 1

For $a_0 = a_1 = 344$ M/S

$P_0/P_1 = 5.03 \times 10^{12}$

$= 1.4$

The unique solution to equations 1 through 6 is:

$M_S = 3.0144$	$M_3 = 104.1$
$U_2 = 769$ M/S	$U_3 = U_2$
$P_2/P_1 = 10.4$	$P_3/P_1 = P_2/P_1$

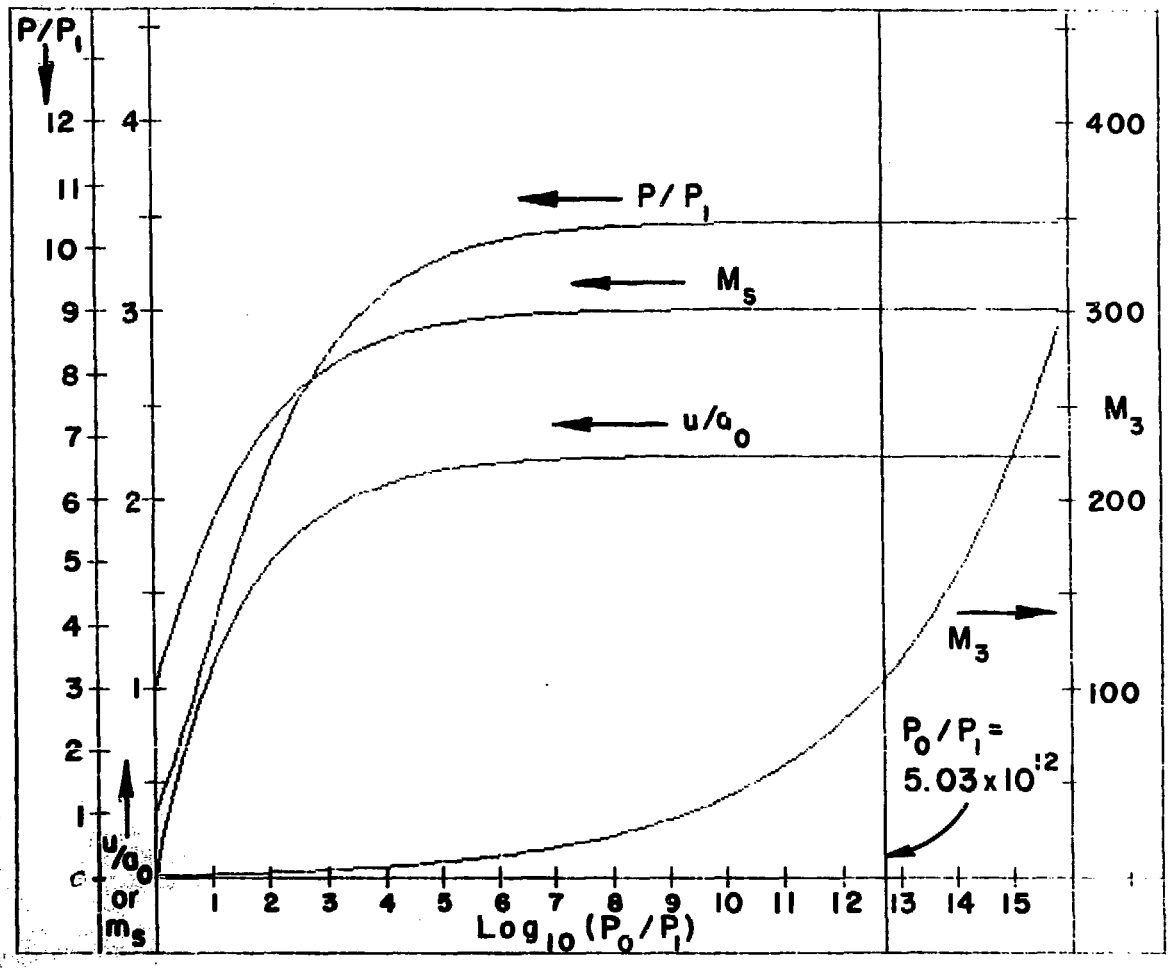
P/P1
12
11
10
9
8
7
6
5
4
3
2
1
0
4
3
2
1
u/a0
or
ms
1
2
3
4
5
6
7
8
9
10
11
12
13
14
15
Log10 (P0/P1)
P/P1
Ms
u/a0
M3
P0/P1 =
5.03x10^12
400
300
200
100
M3

Figure 4

normalized contact surface pressure, normalized contact surface velocity, region 3 flow Mach number, and the shock Mach number all plotted against the diaphragm pressure ratio. Figure 4 also shows the solution for the existing diaphragm pressure ration of 5.03×10^{12}. One interesting observation from figure 4 is that the solution demonstrates asymptotic behavior at a relatively low diaphragm pressure ratio compared to the existing ratio (10^6 versus 10^{12}). Of course M_3 is unbounded because from the isentropic one-dimensional energy equation:

$$\frac{U_3^2}{2} + \frac{a_3^2}{\gamma - 1} = \frac{a_0^2}{\gamma - 1} \qquad \text{(isentropic)} \tag{7}$$

as

$$a_3 \to 0 \quad , \quad U_3 \to \sqrt{\frac{2}{\gamma - 1}}\, a_0$$

and

$$M_3 \to \infty$$

IV. Beam Line Area Discontinuities

Oppenheim and Urtiew[2] describe the interaction of a travelling shock with a single area discontinuity. Depending on the incident shock Mach number and the ratio of areas there are some nine possible results. These are solutions "in the large", i.e., at times sufficiently large so that local interaction effects have died out and isentropic expansions have fanned out to neglible strength. For reasons discussed in Appendix B we shall not attempt to utilize this theory here. Instead we shall treat an area discontinuity as a smooth nozzle. As the flow approaches the nozzle the

flow is choked, at times sufficiently large the flow has again stablized and is now either choked at the new area (if it is less than the old area) or is supersonic, i.e., it has been expanded past a throat depending on whether the flow has encountered an area convergence or divergence respectively (see figure 5).

Case 1 Convergence (Figure 5a)

The flow enters the nozzle area A_1 choked. At times large enough to justify the assumption of quasi-steady one-dimensional flow, the flow is choked at A_2 where $A_2 < A_1$. The flow upstream of the nozzle is now subsonic. Clearly some signal has propagated upstream and induced on incremental velocity in the negative direction. Since the signals from the area contraction must travel upstream at a speed greater than the local sound speed the signals must constitute a shock propagating upstream. Note that from figure B.1 a shock is propagated upstream of an area convergence for all but area ratios near one and large incident Mach numbers. However, we ignore the existence of such shocks and the time required for the flow to stablize to choked flow at a smaller throat area.

Case 2 Divergence (Figure 5b)

In this case the flow is accelerated to a Mach number greater than one. Of course the flow is still choked at A_1.

V. Beam Line Flow Results

Again it should be kept in mind that this analysis assumes quasi-steady one dimensional flow. Also, isentropic flow has to be assumed in order to yield worst case estimates of the flow behavior; in particular the pressure loading. Table 2 contains the pertinent data to be used to calculate the flow Mach number in each of the sections.

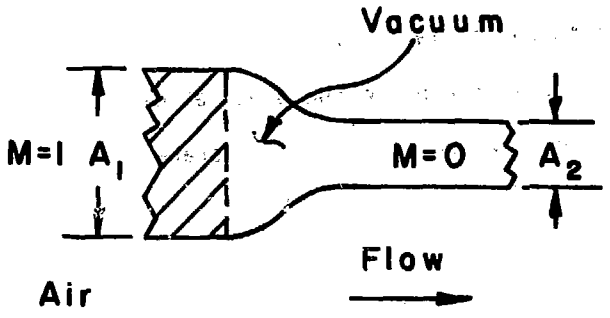

Before interaction

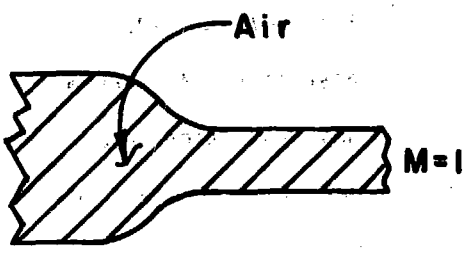

After interaction

(a) Convergence

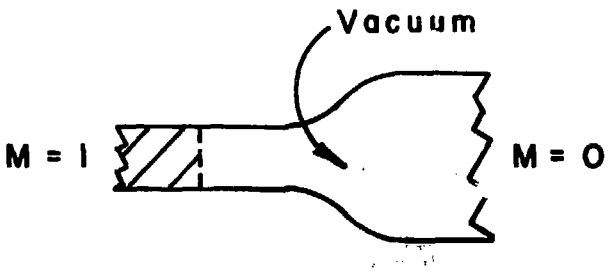

Before interaction

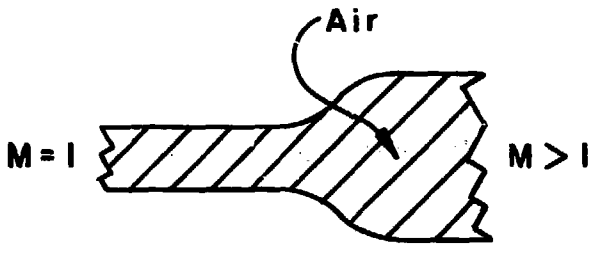

After interaction

(a) Divergence

AREA DISCONTINUITIES

FIGURE 5

Figure 6 is a plot of the information contained in Table 2. With our assumption of isentropic one-dimensional flow one can use the area ratios and stagnation reservoir conditions to calculate the thermodynamic state variables at every section and the mass flow rate. The mass flow rate is given by:

$$(8) \qquad \dot{m} = \frac{P_0}{\sqrt{T_0}} \left[\frac{\gamma}{R} \left(\frac{2}{\gamma + 1} \right)^{\frac{\gamma+1}{\gamma-1}} \right]^{1/2} A_*$$

with

$$P_0 = 1.01 \times 10^5 \ N/M^2 \qquad T_0 = 295K$$

$$A_* = A_c = 5.47 \times 10^{-3} \ M^2$$

This yields

$$\dot{m} = 1.30 \ KG/S$$

The exit Mach number is given by an iterative solution of:

$$(9) \qquad \frac{A}{A_*} = \frac{1}{M_{exit}} \left[\frac{2}{\gamma + 1} \left(1 + \frac{\gamma - 1}{2} M_{exit}^2 \right) \right]^{\frac{\gamma+1}{2(\gamma-1)}}$$

For $A/A_* = 2.32$ the solution of equation (9) is:

$$M_{exit} = 2.36$$

Table 2

Beam Line Area Data

Section	Cross-Sectional Area (M^2)	Length M	Location M
A	8.66×10^{-3}	5.03	$0 < R < 5.03$
B	8.17×10^{-3}	2.13	$5.03 < R < 7.16$
C	5.47×10^{-3}	1.52	$7.16 < R < 8.68$
D	1.27×10^{-2}	1.02	$8.68 < R < 9.70$

	A/A_c[1]	Mach Number	$r = R/R_o$[2]
A	1.58	.403	$0 < r < .52$
B	1.49	.434	$.52 < r < .74$
C	1.00	1.00	$.74 < r < .89$
D	2.32	2.362	$.89 < r < 1.00$

Notes:

1. Area normalized to the area of Section C.
2. Distance normalized to the right end of Section D.

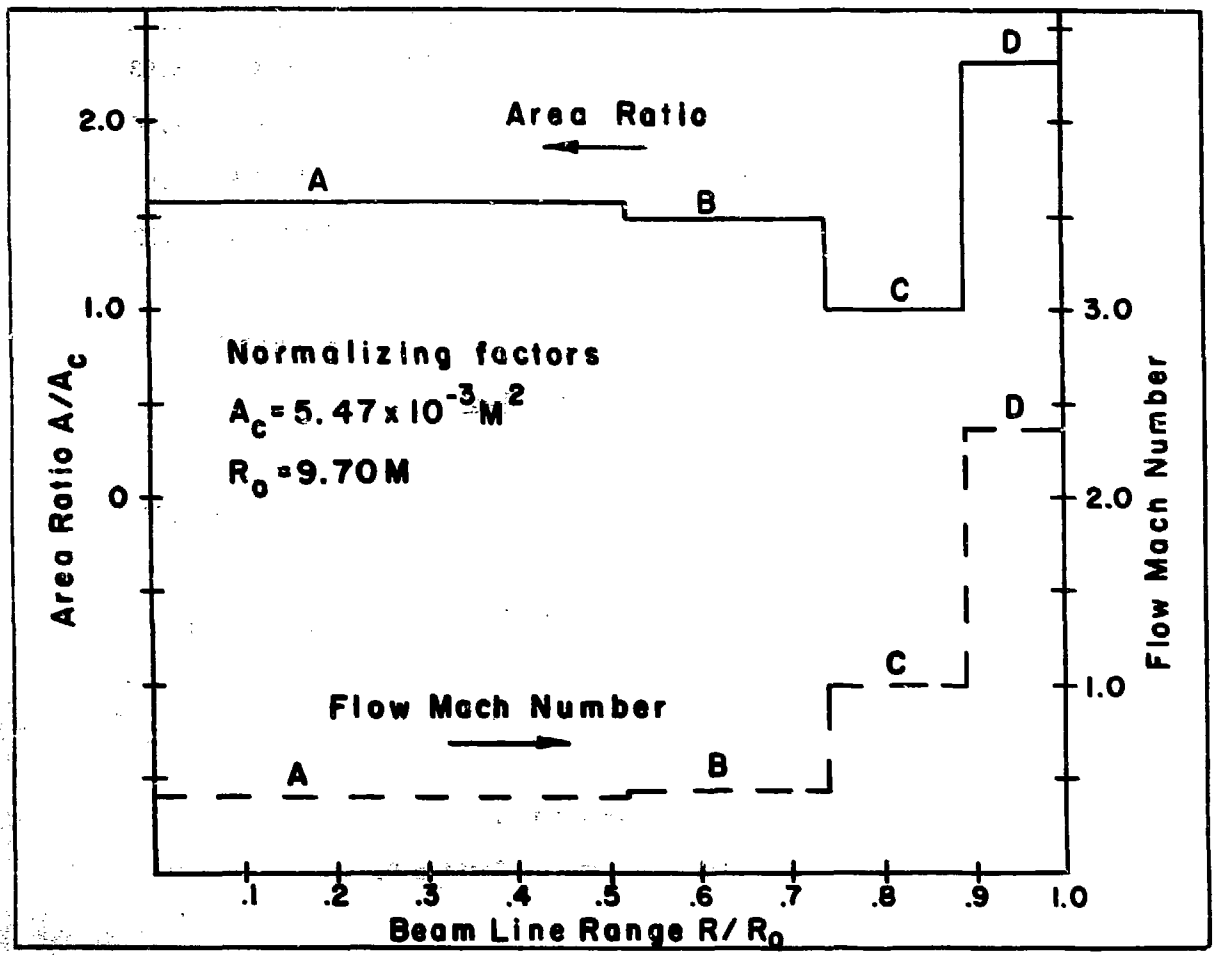
Area Ratio
Flow Mach Number
A
B
C
D
Normalizing factors
$A_c = 5.47 \times 10^{-3} M^2$
$R_0 = 9.70 M$
Area Ratio A/A_c
Flow Mach Number
Beam Line Range R/R_0
2.0
1.0
0
3.0
2.0
1.0
.1
.2
.3
.4
.5
.6
.7
.8
.9
1.0

Figure 6

These data are to be used as inputs to the second part of the solution, i.e., the flow of air into Sectons D and E. Note from figure 1 that Section E has as its left boundary the fragile cryopanel.

Figure 6 also shows the flow Mach number attained from equation 9 for each area ratio.

VI. Flow to Cryopanel

The one-dimensional flow at the exist of section D is now allowed to expand spherically into section E. Figure 7 is a detail of the sections D-E juncture.

We continue to use one-dimensional flow equations by breaking the flow at the exit of section D into an arbitrarily large number of stream tubes. Then each stream tube contributes proportionately to the spherical surface area.

From the elevation view of figure 7 we note that assuming cylindrical rather than spherical expansion involves a negligible error because of the confining surfaces. When the gas particles just begin to impinge upon the cryopanel the radius of the cloud is 114 mm (see figure 7). The area A(r) is equal to the sum $A_1 + A_2$ where:

$$A_1 = w \times h$$

$$w = 127 \text{ mm}$$

$$h = 178 \text{ mm}$$

$$A_1 = 2.26 \times 10^{-2} \text{ M}^2$$

and

$$A_2 = \frac{\pi}{2} \times r \times h$$

$$r = 114 \text{ mm}$$

$$h = 178 \text{ mm}$$

$$A_2 = 3.19 \times 10^{-2} \text{ M}^2$$

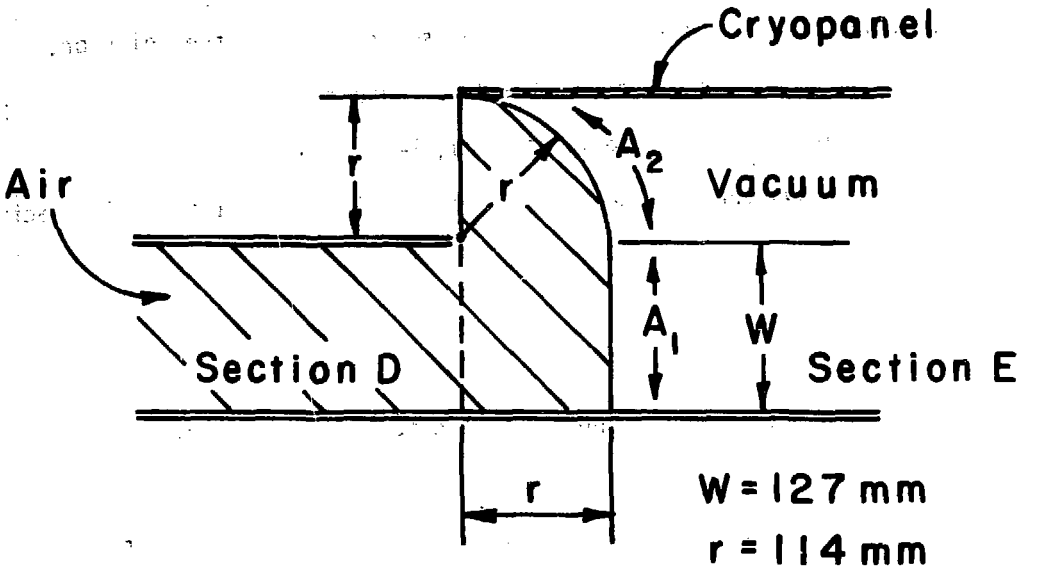

(a) Plan View

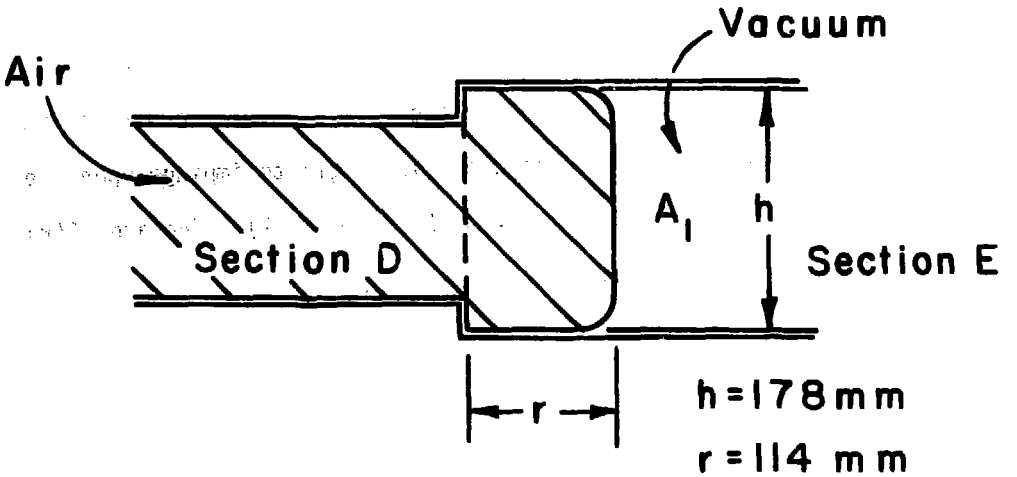

(b) Elevation View

1-d to 3d TRANSITION

Figure 7

A (r = 114 mm) = 5.45×10^{-2} M^2. If we distribute this area equally over each stream tube, then each has undergone an area expansion of:

$$\frac{A(r = 114)}{A_D} = 4.92$$

With this area ratio and the choked flow restriction at $A_* = A_c = 5.47 \times 10^{-3}$ M^2 we can determine the Mach number of the flow just as it impinges upon the cryopanel.

$$\frac{A(r = 114)}{A_*} = \frac{A(r = 114)}{A_D} \times \frac{A_D}{A_*} = 11.4$$

Solving equation 9 interatively yields a flow Mach number of 4.07. We shall now use this result, the energy equation for one-dimensional steady isentropic flow, and other shock relations to calculate the initial pressure loading due to the reflected shock.

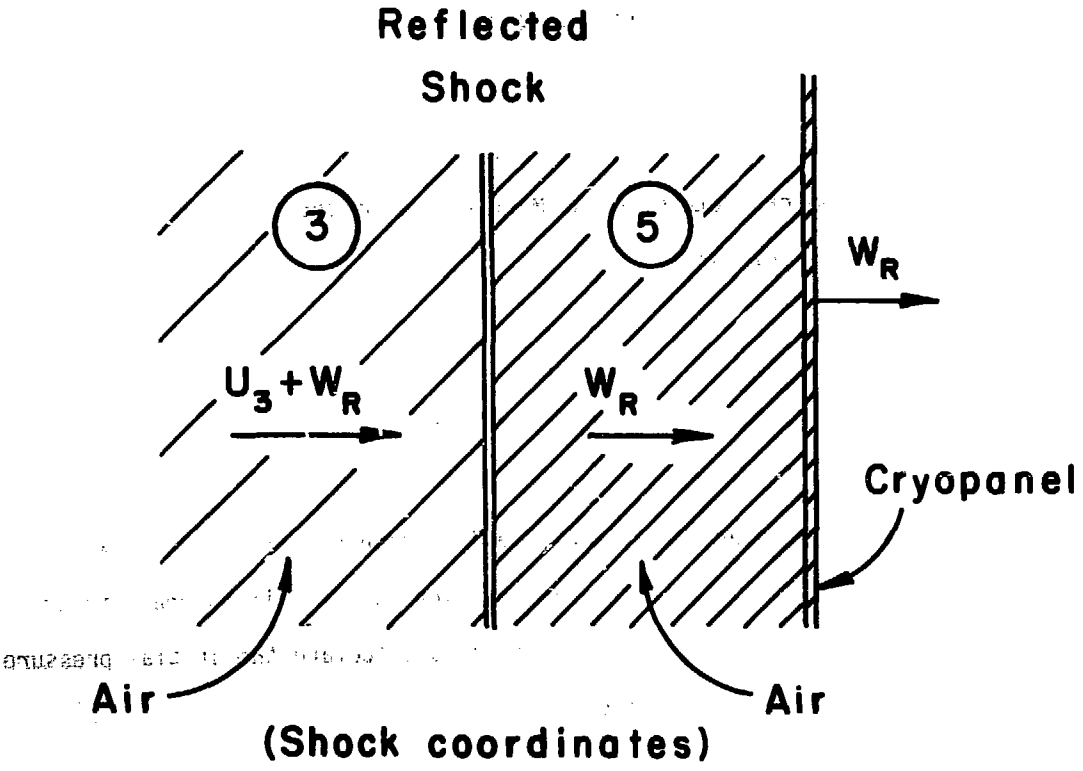

REFLECTED PRESSURES ON CRYOPANEL

Figure 8

VII. Initial Cryopanel Pressure Loading

Figure 8 shows the shock that is reflected from the cryopanel. In these shock-fixed coordinates conservation of mass yields:

$$\frac{\rho_5}{\rho_3} = \frac{U_3 + W_R}{W_R} \tag{10}$$

where W_R is the shock velocity in laboratory coordinates. For a shock we also have:

$$\frac{\rho_5}{\rho_3} = \frac{(\gamma + 1)M_R^2}{(\gamma - 1)M_R^2 + 2} \quad \text{(shock)} \tag{11}$$

The value of a_3 is given by:

$$a_3 = a_0 \left(1 + \frac{\gamma - 1}{2} M_3^2\right)^{-1/2} \quad \text{(isentropic)} \tag{12}$$

and (with $M_3 = 4.07$)

$$U_3 = M_3 a_3 = 674 \text{ M/S} \tag{13}$$

Using these values equations 10 and 11 can be solved iteratively yielding a reflected Mach number of (M_R=) 2.15. We now can solve for the static pressure in region 5. From the isentropic flow relations:

$$\frac{P_3}{P_0} = \left(1 + \frac{\gamma - 1}{2} M_3^2\right)^{\frac{-\gamma}{\gamma-1}} = 6.00 \times 10^{-3} \quad \text{(isentropic)} \tag{14}$$

From the normal shock relations:

$$(15) \qquad \frac{P_5}{P_3} = 1 + \frac{2\gamma}{\gamma + 1}(M_R^2 - 1) = 5.23 \qquad \text{(shock)}$$

therefore $$\frac{P_5}{P_0} = \frac{P_5}{P_3} \times \frac{P_3}{P_0} = 3.14 \times 10^{-2}$$

The intial pressure loading on the cryopanel is 3.17×10^3 N/M^2 or 23.9 Torr. Compared to the atmospheric reservoir pressure this is quite low. Compared to the extremely high vacuum (2×10^{-8} N/M^2) into which the air is flowing this is a very large pressure jump. The pressure on the far side of the cryopanel is near zero relative to P_5. Therefore P_5 can be used to calculate the initial loading of the cryopanel. The pressure loading on the cryopanel will increase with time due to several effects. First, the initial reflected shock will be reflected back to the cryopanel. Second, as more mass flows into the tangent tank the pressure will increase because of the increasing density. Because of the large tangent tank volume and the relatively low mass flow rate of 1.3 Kg/S this is a late time effect.

VIII. Flow Times

From the shock solution presented in table 2 the time required for the initial shock to travel to the end of the beam line (R=9.7 meters) is

$$(16) \qquad t_s = \frac{9.70}{M_s a_1} = 9.35 \text{ ms}$$

where M_s=3.01 and a_1=344 M/S

The time required for the contact surface to travel 9.7 meters is

$$(17) \qquad t_{cs} = \frac{9.70}{U_2} = 12.61 \text{ ms}$$

where U_2 = 769 M/S

The time required for the front of our choked flow solution is the sum of the flow times for each section. The flow in sections A through C is at M = 1. Therefore (using the table 2 data):

$$t_{A-C} = \frac{8.68}{a_1} = 25.23 \text{ mS}$$

The flow through section D is

$$t_D = 1.26 \text{ mS}$$

where $M_D = 2.36$

$$t_{Total} = t_{A-C} + t_D = 26.49 \text{ mS}$$

Whether or not fast-acting valves can be designed to operate within these time constraints is currently under investigation.

IX. Dicussion Of The Results

This is a very conservative analysis and should provide a reasonable upper bound for the early time (relative to the flow transit time) behavior.

The rigorous solution presented in table 1 and figure 4 exhibits the asymptotic behavior that one would expect considering the very low pressures into which the shock is propagating.

The modelling of the area discontinuities as isentropic nozzles is especially conservative in that the entropy produced by the large number of shocks that would by produced by the four discontinuous area changes would be substantial.

Appendix A: Knudsen Number Calculation

A rarefied gas flow is a flow in which the molecular mean free path λ is comparable to some significant dimension L of the flow field[1]. The gas then exhibits some characteristics of its course molecular structure. The dimensionless ratio

$$K = \frac{\lambda}{L} \tag{A.1}$$

is called the Knudsen number. For hard sphere molecules having a maxwellian velocity distribution, the mean free path is given by[3]

$$\lambda = \frac{1}{\sqrt{2}\,\pi\, N\, d^2} \text{ (meters)} \tag{A.2}$$

where N: number of molecules/M^3

d: molecular diameter (meters)

The ideal gas law can be written as:

$$P = NKT \tag{A.3}$$

where N is as defined above and K is Boltzman's constant (1.38×10^{-23} Joule/K). For a pressure of 2×10^{-8} N/M^2 and a temperature of 295K

$$N = 4.91 \times 10^{12} \text{ molecules/}M^3$$

The value of d for nitrogen at S.T.P. is:

$$d = 3.5 \times 10^{-10} \text{ meters}$$

Equation A.2 yields:

$$\lambda = 3.74 \times 10^{5} \text{ meters}$$

Taking the thickness of section C as our smallest dimension of the beam line:

$$L = .048 \text{ meters}$$

Equation A.1 yields:

$$K = 7.80 \times 10^{6}$$

Generally free molecular flow exists for[1] $K > 3$. With a Knudsen number on the order of 10^6 this flow is clearly in the free molecular flow regime.

Appendix B: Shock-Area Change Interactions

Figure B.1 shows the possible wave systems that can result from the interaction of a travelling shock with a discrete area change. This was taken from reference 2. The straight lines represent shocks, both transmitted and reflected. The dotted lines represent contact surfaces. There are nine regions on figure B.1. The boundaries between the regions are given by implicit relationships between the incident shock Mach number and the area ratio. To use this theory for the present problem would require one to account for an increasing (in time) number of shocks resulting from the four area changes in the beam line. In addition one would have to account for shock-shock and shock-contact surface interactions. These interactions could be of both overtaking and collision interactions.

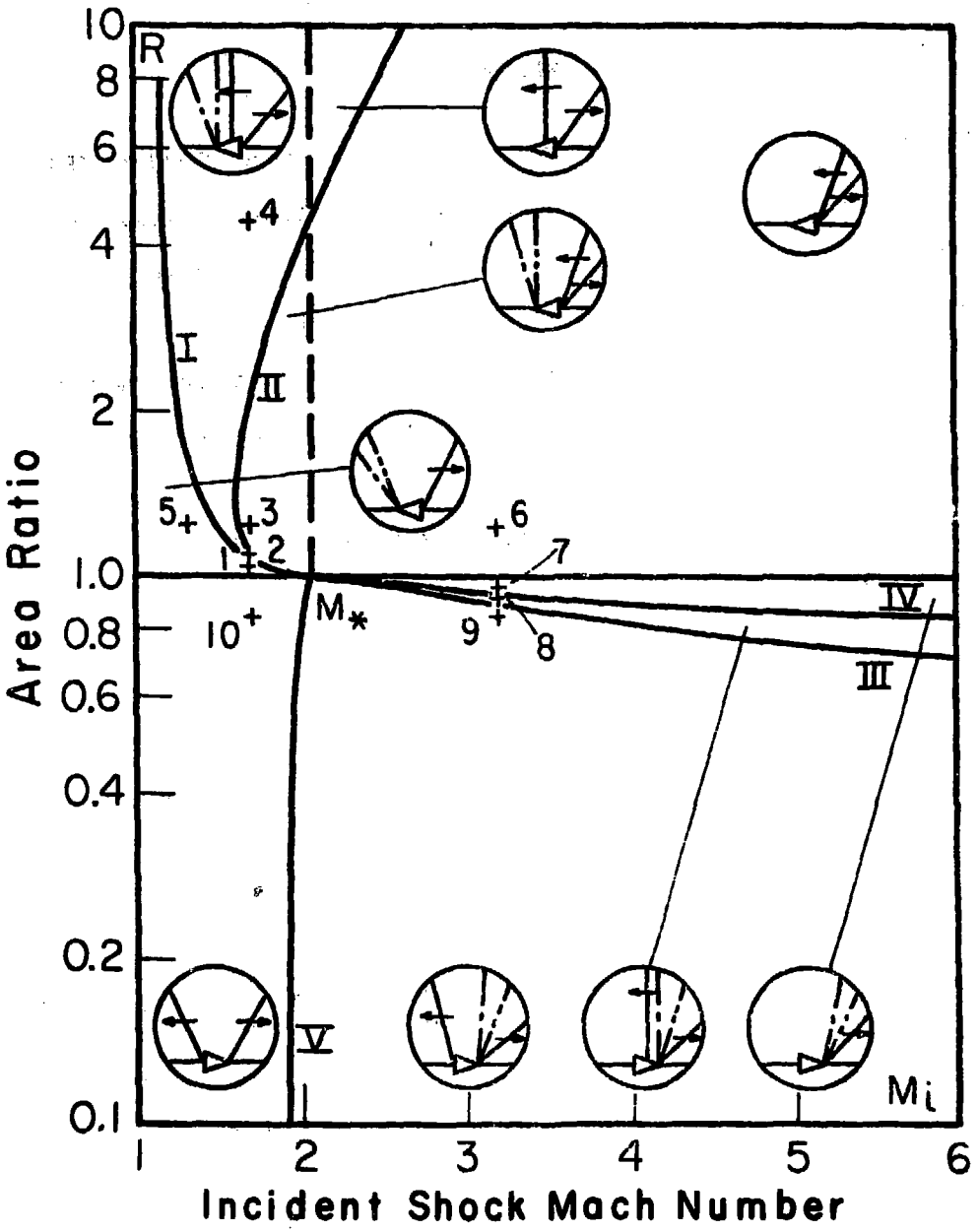

REGIMES OF SOLUTIONS FOR SHOCK INTERACTIONS

WITH SINGLE AREA DISTURBANCES

in the R - M_i plane

FIGURE B.1

Acknowledgements

I would like to thank the U.S. Air Force Weapons Laboratory, Kirtland AFB, NM for providing this opportunity for me to return to school to complete the requirements for an MS degree. The Lawrence Berkeley Laboratory provided an interesting problem and staff support, both technical and administrative. Professors Sherman and Oppenheim, Mechanical Engineering Department, U.C. Berkeley, deserve thanks for their encouragement and technical assistance.

This work was supported by the U. S. Department of Energy under Contract W-7405-ENG-48.

References and Bibliography

1. S. A. Schaaf and P. C. Chambre, "Flow of Rarefied Gases", Princeton University Press 1961, p3.

2. A. K. Oppenheim and P. A. Urtiew "Vector Polar Method for Shock Interactions with Area Disturbances", Univ. of Calif. Technical Note DR4, July, 1959.

3. J. F. Clark and M. McChesney, "The Dynamics of Real Gases", Wiley, New York, 1965; Chapter 2.